GRAVITATIONAL RADIATION FROM THE COLLAPSE AND EXPLOSION OF RAPIDLY ROTATING, HOMOGENEOUS, GASEOUS ELLIPSOIDS IMBEDDED IN HALOS

H. BELTRAMI and W. Y. CHAU

Astronomy Group, Department of Physics, Queen's University at Kingston, Ontario, Canada

(Received 24 July, 1985)

Abstract. The nonlinear motion (collapse/explosion) of a homogeneous, rapidly rotating, gaseous ellipsoid has been studied with the effects of an external gravitational field incorporated. The non-axisymmetric motion has been followed using an efficient numerical code based on certain properties of the potential functions. The gravitational radiation associated with the phenomenon was calculated, and the wave forms studied to extract information on the dynamics of the source. Possible implications of our results for various astrophysical processes are discussed.

1. Introduction

We have extended our earlier work on the collapse and explosion of rapidly rotating, uniform density gaseous spheroids to incorporate the effects of non-axisymmetry and the presence of an external gravitational field. We have also made a detailed study of the gravitational radiation (hereafter to be abbreviated as GR) emitted and the information contained in the wave forms of such radiation.

The basic formulation for describing the problem was completed by Fujimoto (1968) who did not consider, however, either the GR associated with the phenomena or the effects of an external field. The emission of GR has subsequently been studied in the case of axisymmetric collapse by Thuan and Ostriker (1974), Novikov (1975), Chia *et al.* (1977), Shapiro (1977); in the case of non-axisymmetric collapse by Saenz and Shapiro (1978, 1979) and in the case of axisymmetric explosion with/without a magnetic field by Chan *et al.* (1978, 1980) (hereafter referred to as Paper I), and Henriksen *et al.* (1979). The effect of an external gravitational field in such phenomena, however, does not seem to have received any attention.

In the study reported here, we have been able to follow the evolution of the non-axisymmetric configuration with a very efficient numerical code that makes use of some elegant relations among the various potential functions (see Section 2 for details). This should serve as a useful, independent check on the results of Saenz and Shapiro (1978, 1979) for the case of collapse. As a first step for studying some of the effects of an external field, we confine ourselves to the case of a core imbedded in a rigid, axisymmetric halo of different eccentricity and density and assume that the only interaction between the halo and the core is gravitational and that the interpenetration of the halo and core matter has no effects on each other. Such assumptions, though restrictive, are common (see, e.g., Durisen, 1978). Futhermore, there seems to be

Astrophysics and Space Science **119** (1986) 353–372.

evidence that massive, invisible halos do exist around some galaxies between which the only interaction could be gravitational.

The results obtained (see Section 3) are very suggestive for the morphology of star formation regions, and various process like galaxy formation, astrophysical jets and supernova activities. Some of the underlying assumptions should, therefore, be relaxed in future work to allow a more realistic evaluation of the implications.

The paper is organized as follows. The formulation is presented in Section 2, and the results of numerical experiments on the configurations in Section 3. The GR produced and the associated wave forms are computed in Section 4. The results are summarized and possible implications discussed in Section 5.

2. Formulation

The equations of motion and the dynamical properties of a uniformly rotating, homogeneous ellipsoid have been extensively discussed (see, e.g., Fujimoto (1968) for the general case, and Chia *et al.* (1977) for the axisymmetric case). Employing their notations, we can write down the equations of motion, in the absence of an external field, for the uniform ellipsoid of ideal gas, with mass M, density $\rho(t)$, central pressure $P_c(\rho)$, angular momentum $\frac{2}{5}ML$ (assumed to be equal to the circulation), and semi-major axes $a_i(t)$ ($i = 1, 2, 3$ with the 3- or z-axis along the rotational axis) as

$$\frac{\mathrm{d}^2 a_1}{\mathrm{d}t^2} = -2a_1 A_1 + \frac{2P_c}{\rho a_1} + \frac{8L^2}{(a_1 + a_2)^3}\,, \tag{1}$$

$$\frac{\mathrm{d}^2 a_2}{\mathrm{d}t^2} = -2a_2 A_2 + \frac{2P_c}{\rho a_2} + \frac{8L^2}{(a_1 + a_2)^3}\,, \tag{2}$$

$$\frac{\mathrm{d}^2 a_3}{\mathrm{d}t^2} = -2a_3 A_3 + \frac{2P_c}{\rho a_3}\,; \tag{3}$$

where, of course, $M = 4\pi/3\ \rho a_1 a_2 a_3$, and the A_i's are Lamé functions (Chandrasekhar, 1969) defined by

$$A_i = \frac{3GM}{4} \int_0^\infty \frac{\mathrm{d}s}{\Delta(a_i^2 + s)} \tag{5}$$

with

$$\Delta^2 = (a_1^2 + s)(a_2^2 + s)(a_3^2 + s)\,. \tag{6}$$

The central pressure P_c is related to the central temperature T_c by

$$P_c = \frac{\rho}{\mu m_H}\, kT_c\,, \tag{7}$$

where the symbols have their usual meanings. The formulation is now completed by the following assumed cooling law (Fujimoto, 1968; Chia *et al.*, 1977)

$$\frac{dT_c}{dt} + \frac{2}{3} T_c \frac{d}{dt} \ln(a_1 a_2 a_3) = -\kappa \rho T_c ; \tag{8}$$

with κ being an arbitrary constant.

The gravitational effect of the halo which is assumed here to be concentric, rigid, non-responsive, interpenetrating, spheroidal, and of uniform density can be readily incorporated (see, e.g., Durisen, 1978). It consists of, in the end, simply replacing the A_i's in Equations (1)–(3) by the ones appropriate for the combined halo–core system

$$A_i \to A_i + A_i' - A_i'' , \tag{9}$$

where A_i is given as before by Equations (5) and (6), A_i' is the corresponding expression for the whole halo (i.e., mass M' and semi-major axis a_i') while A_i'' is that for the portion of the halo occupying the core's volume (i.e., mass $M'' = M'(a_1 a_2 a_3 / a_1' a_2' a_3')$ and semi-major axes a_i).

Certain properties of the Lamé functions prove to be very useful in the solution of the problem. In the case of axial symmetry, we have for an oblate object ($a_1 = a_2 \geq a_3$),

$$\begin{aligned} A_1 &= \frac{3GM}{4} \frac{1}{a_1^3 e^3} [\sin^{-1} e - e\sqrt{1-e^2}] , \\ A_3 &= \frac{3GM}{4} \frac{1}{a_1^3 e^3} \left[\frac{e}{\sqrt{1-e^2}} - \sin^{-1} e \right] , \end{aligned} \tag{10}$$

with

$$e^2 = 1 - \frac{a_3^2}{a_1^2} ;$$

while for a prolate object ($a_1 = a_2 \leq a_3$)

$$\begin{aligned} A_1 &= \frac{3GM}{4} \frac{1}{a_1^2 a_3} \left[\frac{1}{e^2} - \frac{1-e^2}{2e^3} \ln\left(\frac{1+e}{1-e} \right) \right] \\ A_3 &= \frac{3GM}{4} \frac{1}{a_1^2 a_3} \left[\frac{1-e^2}{e^3} \ln\left(\frac{1+e}{1-e} \right) - \frac{2(1-e^2)}{e^2} \right] \end{aligned} \tag{11}$$

with

$$e^2 = 1 - \frac{a_1^2}{a_3^2} .$$

For the general case, the A_i's are given by the incomplete elliptical integrals of both types. While there is no difficulty in principle involved in evaluating the quadrature, the

necessity for doing this at every step of a long calculation would render the whole computation excessively time consuming. Instead, we make use of the following theorem for the Lamé functions (see, e.g., Fujimoto, 1968):

$$\frac{\mathrm{d}A_i}{\mathrm{d}t} = -\left(3a_i A_{ii}\frac{\mathrm{d}a_i}{\mathrm{d}t} + \sum_{j\neq i} a_j A_{ij}\frac{\mathrm{d}a_j}{\mathrm{d}t}\right), \tag{12}$$

where the 2-index symbols A_{ij}'s are define by

$$A_{ij} = \frac{3GM}{4}\int_0^\infty \frac{\mathrm{d}\mu}{\Delta(a_i^2+\mu)(a_j^2+\mu)}, \tag{13}$$

and are related to the A_i's by (Chandrasekhar and Levobitz, 1962)

$$A_{ij} = -\left(\frac{A_i - A_j}{a_i^2 - a_j^2}\right), \quad i\neq j. \tag{14}$$

Furthermore, we have

$$2A_{ii} + \sum_{i=1}^{3} A_{ji} = \frac{2}{a_i^2 a_1 a_2 a_3}\left(\frac{3GM}{4}\right). \tag{15}$$

In principle then, one will solve Equation (12) (for $i = 1, 2, 3$ with the help of Equations (14) and (15)) in conjunction with Equations (1), (2), (3), and (8) and one can avoid calculating the elliptical integrals at every step of the computation. Care has to be exercised, however, when any of the axis approaches one another, for it will become difficult to evaluate A_{ij} using Equation (14).

As an illustration, consider the case in which all axes approach the same value – i.e., a nearly spherical configuration with, say, $a_1 = a_3(1+\alpha)$, $a_2 = a_3(1+\varepsilon)$ and $\alpha, \varepsilon \ll 1$. We can then obtain from Equation (13) by the expansion

$$A_{12} = A_{33} - 3a_3^2(\varepsilon+\alpha)A_{333}, \tag{16}$$

$$A_{13} = A_{33} - a_3^2(3\varepsilon+\alpha)A_{333}, \tag{17}$$

$$A_{23} = A_{33} - a_3^2(\varepsilon+3\alpha)A_{333}; \tag{18}$$

where the 3-index symbols A_{ijk} are defined by

$$A_{ijk} = \frac{3GM}{4}\int_0^\infty \frac{\mathrm{d}\mu}{\Delta(a_i^2+\mu)(a_j^2+\mu)(a_k^2+\mu)}. \tag{19}$$

They can be simply deduced from the A_{ij}'s when all the indices are not the same by the relations (Chandrasekhar and Lebovitz, 1962)

$$A_{ijk} = -\frac{A_{ij} - A_{ik}}{a_j^2 - a_k^2}, \quad j\neq k, \qquad A_{ijk} = -\frac{A_{ji} - A_{jk}}{ai^2 - a_k^2}, \quad i\neq k. \tag{20}$$

When all the indices are the same, we can make use of the relation

$$2A_{iij} + 2A_{ijj} + \sum_{k=1}^{3} A_{ijk} = \frac{2}{a_1 a_2 a_3 a_i^2 a_j^2} \quad . \tag{21}$$

For the near spherical configurations we are considering, $a_1 \to a_3$, $a_2 \to a_3$, Equations (15) and (21) then readily yields

$$A_{33} = \left(\frac{3GM}{4}\right)\frac{2}{5a_3^5} \tag{22}$$

and

$$A_{333} = \left(\frac{3GM}{4}\right)\frac{2}{7a_3^7} \tag{23}$$

to be used in Equations (16)–(18).

In the case of a near-axisymmetric configuration, similar considerations apply. Thus for $a_2 = a_1(1 + \varepsilon)$, we have

$$A_{12} = A_{11} - 3a_1^2 \varepsilon A_{111} \,, \tag{24}$$

where A_{11} can be readily calculated from (14) and (15) and A_{111} from (20) and (21).

3. Numerical Solutions: Geometric Evolution of the System

The equations governing the evolution of the system, Equations (1), (2), (3), (8), and (12) are rendered dimensionless by scaling identical to that used in Paper I. Specifically, the units for length, time, temperature are $a_1(0)$, $[4a_1^3(0)/3GM]^{1/2}$, and $[3GM\mu M_H/8ka_1(0)]$, where the bracketed zero refers to the initial values of the quantity involved. The starting configuration is always assumed to be axisymmetric and hence the axis (dimensionless) are determined for a given accentricity $e(0)$. The values of L and $T_c(0)$ are expressed in terms of the equilibrium values given by Equations (1) and (3):

$$T_{c,e}^* = 2a_3^* A_3^* \,, \tag{25}$$

$$L_e^* = [2a_1^{*2}(a_1^{*2}A_1^* - a_3^{*2}A_3^*)]^{1/2} \,, \tag{26}$$

where the *-quantities are dimensionless.

A typical numerical run is then initiated by assigning values for $e(0)$, κ, L, and $T_c(0)$ and the velocities of the axis (physical quantities can be recovered when, e.g., $a_1(0)$ and M are specified.) The computation is terminated for the case of collapse when (a) any of the axes reaches the Schwarzschild radius, and/or (b) the velocity reaches that of light, and/or (c) the central temperature becomes negative. For the case of explosion, the computation is carried out to ~ 100 units of time or when the system has clearly attained a steady configuration. It is clear that a thorough sampling of the (4) parameter space would be timewise-prohibitive. Fortunately, typical, representative cases have

been presented by Fujimoto (1968) for the case of collapse and by Chan *et al.* (1978) for the case of explosion. Since our interest is on the additional effects of non-axisymmetry and external gravitational field, our choice of the starting conditions is, therefore, guided by the two works just referred to.

3.1. Collapse: no external field

This situation has been throughly studied by Fujimoto (1968) for the general case, and by Chia *et al.* (1977), and Shapiro (1977), for the axisymmetric case with the emission of GR. This is repeated here first as a check on the numerical scheme, the accuracy of which is indeed confirmed by the results of our calculation for a non-axisymmetric collapse (Figure 1) which can be seen to be identical to those of Fujimoto's for the corresponding case with similar initial conditions. Of more importance, we shall also try to relate the results to some actual, realistic astrophysical situations.

The interesting result coming out of these computations, as was already observed by Fujimoto (1968), is that a small non-axisymmetric perturbation applied to an initially axisymmetric system could lead to a later configuration which is extremely elongated. The effect is much more pronounced for large angular momentum. In the typical case presented (Figure 1), the non-axisymmetric perturbation has a kinetic energy $\sim 1.8 \times 10^{-3}$ that of rotation, the angular momentum is four times the equilibrium one and the configuration arrived at after 6τ has a ratio of 0.85 : 1.31 : 0.21 for $a_1 : a_2 : a_3$. A similar case with only the difference of $L = L_e$ results in a ratio of only 0.2 : 2 : 0.1 $\sim 1.2\tau$.

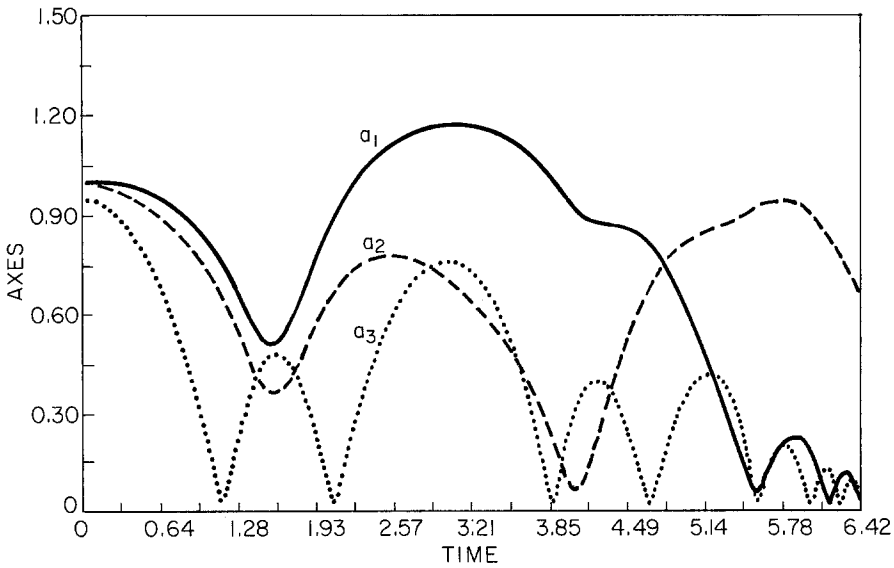

Fig. 1. Non-adiabatic, non-axisymmetric collapse. The initial parameters are $L = 4L_e$, $T_c(0) = 0.111T_{c,e}$, $e(0) = 0.31225$, $k^* = 0.01$ A small non-axisymmetric perturbation has been applied to the equatorial axes $da_1/dt(0) = -da_2/dt(0) = 0.04$. Time is in units of τ and axes in units of $a_1(0)$.

Although the 'final' steady configuration cannot really be discussed within the present framework, the results appear nonetheless extremely suggestive for various processes like formation of barred galaxies, close binaries and the morphology of certain star formation regions. Here, we will illustrate the possible significance of our results by considering a typical molecular cloud of mass $M = 160\,M_\odot$ and density $\rho \sim 1.2 \times 10^{-20}\,\mathrm{g\,cm^{-3}}$ (Bock, 1977; Field, 1978). With the parameters used in Figure 1, this then determines $a_1(0) = a_2(0)$, and $a_3(0)$ for our system. The angular momentum used would then be $L \sim 9 \times 10^{-24}\,\mathrm{cm^2\,s^{-1}}$, in reasonable agreement with the value of $\sim 2 \times 10^{-24}\,\mathrm{cm^2\,s^{-1}}$ reported by Bodenheimer and Black (1978). Our initial input temperature corresponds to $T_c \sim 10$ K, agreeing with the typical values of ~ 10 K reported by Martin and Barret (1978) and Myers (1983). Our calculations would show then, with an initial non-axisymmetric perturbation as used in Figure 1, that the system would collapse to an elongated shape of $(a_1, a_2, a_3 = 1.85, 0.03, 0.74)$ in $\sim 1.3 \times 10^7$ yr for $\kappa = 0$; (1.1, 0.07, .038) in $\sim 7 \times 10^6$ yr, for $\kappa = 0.005$ and (0.0067, 0.65, 0.0068) in $\sim 4 \times 10^6$ yr for $\kappa = 0.01$. We emphasize again that the results are only suggestive and a much better model than ours is necessary to take into account the complicated but extremely important cooling processes in a collapsing cloud.

3.2. Explosion: no external field

The typical situations for axisymmetric explosion explored by Chan *et al.* (1978) have been re-examined with the inclusion of an initial non-axisymmetric perturbation. These situations correspond to (i) a large initial deposit of energy; (ii) the system being radiation dominated; and (iii) a moderate value for energy and angular momentum, so that the system becomes unbound along the z-axis but oscillates in the $(x - y)$-directions. It was found that with the same small initial, non-axisymmetric perturbation energy ($\sim 0.2\%$ that of rotation) as for the case of collapse, and with $\kappa = 0$, the evolution is hardly different from that of the axisymmetric case. It seems that the decrease in density with the explosion, and the correspondingly reduced gravitational field, conditions opposite to those for collapse, impedes the growth of the perturbation. With the inclusion of thermal energy dissipation ($\kappa = 0.01$), the system does achieve a high degree of tri-axiality, but then the thermal dissipation actually causes a recollapse of the system and, hence, the situation does not really correspond to a pure explosion.

Attempts have been made to determine how large the initial, non-axisymmetric 'kick' has to be to produce a final, significantly asymmetric configuration. It was found that the perturbation energy has to be ~ 6–7 times that of rotation before we can have the desired result (see Figure 2). Possible relevance of this to actual astrophysical situations remains to be investigated.

3.3. Collapse and explosion: effect of an external field

The restrictive assumptions on the nature of the core-halo interactions make it possible to predict the effect of the external gravitational field. With ram-pressure effects omitted, an oblate halo would lead to a flattening of the core along the rotational axis and an expansion on the equatorial plane. A prolate halo, on the other hand, should have just

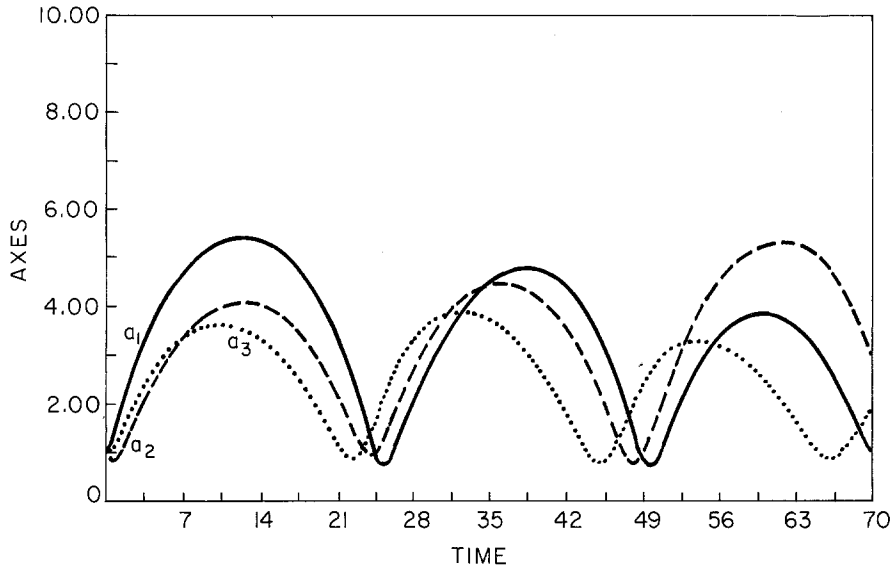

Fig. 2. Non-axisymmetric, adiabatic explosion. The initial parameters are $L = 1.0L_e$, $T_c(0) = 1.5T_{c,e}$, $e(0) = 0.1$, $k^* = 0$. A large non-axisymmetric perturbation has been applied to the axes on the equatorial plane, $da_1/dt(0) = -da_2/dt(0) = 0.5$. Time is in units of τ an axes in units of $a_1(0)$.

the opposite effects. These are indeed confirmed by numerical experiments. Furthermore, we would *not* expect any significant effects for the case of collapse, since the core density and, hence, gravitational field, would increase and rapidly dominate over that of the halo. This is also confirmed by results of the computation.

Our system, then, cannot be used to model the explosion of galaxies imbedded in a tenuous, gaseous medium, an otherwise attractive investigation with possible implications for jets in radio sources. However, our calculations could take on great significance if it is indeed true that many galaxies (especially spirals) are imbedded in a massive, invisible halo (see, e.g., Rubin, 1983) made up of matter (e.g., neutrinos) that essentially only interacts with the visible matter gravitationally. We thus consider the case of an exploding/collapsing galactic size spheroid imbedded in a large, massive halo (mass $\sim 10^{13}$ ⊙, size ~400 kpc) and the results of the computation are presented in Figures 3 and 4. It is clear from Figures 3 and 4 that the rigid spheroidal halo has its main effect on the axes of the equatorial plane. For the case of explosion, ($\rho/\rho' \sim 2.4$), the prolateness of the expanding configuration for $\rho' = 0$ is completely eliminated and the configuration tends towards a flattened shape. As expected, the axes a_1 and a_2 expand, but the non-axisymmetric perturbation does not grow.

For the case of collapse ($\rho/\rho' \sim 10$) the differences with the $\rho' = 0$ case also appear on the equatorial plane. The strongly elongated shapes achieved during non-axisymmetric collapse without halo are clearly reduced. The precise moment when the differences appear seems to be when one of the equatorial axes reaches a large value. In general we can say for collapse that the presence of an external gravitational field does not

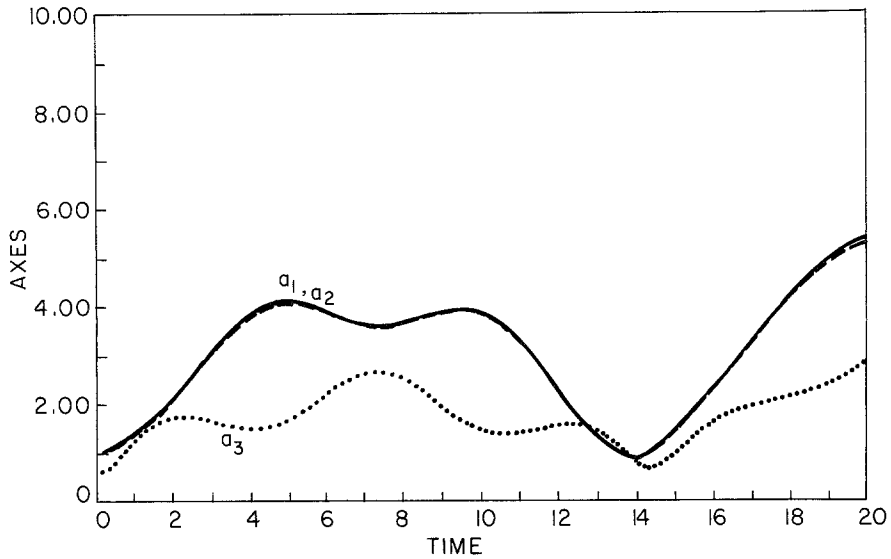

Fig. 3. Effect of external field on a non-axisymmetric explosion. The initial parameters are $l = 0.04L_e$, $T_c(0) = 2.3T_{c,e}$, $e(0) = 0.8, k^* = 0, \rho/\rho' = 2.41, a_1' = a_2' = 15a_1(0)$, and $a_3' = 14a_3(0)$. Time is in units of τ and axes in units of $a_1(0)$.

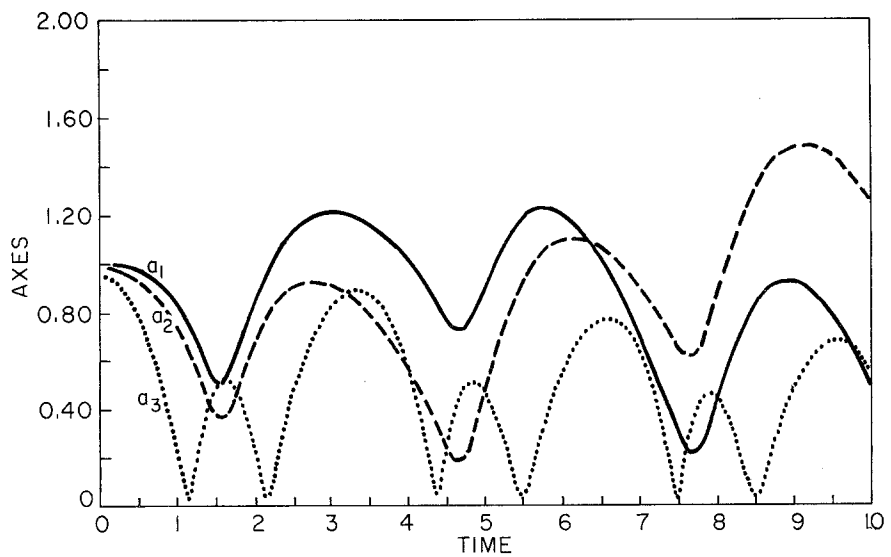

Fig. 4. Effects of an external field on a non-axisymmetric collapse. The initial parameters are $L = 4.0L_e$, $T_c(0) = 0.111T_{c,e}$, $e(0) = 0.31225, k^* = 0$, $\rho/\rho' = 10$, $a_1' = a_2' = 100a_1(0)$, and $a_3' = 80a_3(0)$. Time is in units of τ and axes in units of $a_1(0)$.

contribute to enhanced asymmetries if the halo's density is within one order of magnitude of that of the core. For lower halo densities there are no effects on the evolution of the collapsing configuration.

4. Numerical Solutions: Gravitational Radiation

In this section, we will present the results of our calculations on the gravitational radiation associated with the various situations discussed in Section 3. Since the radiation is general relativistic effect depending critically on the compactness of the system and the shortness of the relevant time-scale, we would therefore expect the amount to be significant only for collapsing situation. Furthermore, as discussed in Section 3, the effects of the halo would then be insignificant.

4.1. Energy loss via gravitational radiation

We assume that the rate of gravitational radiation is given (cf. Landau and Lifshitz, 1975) by

$$\frac{\mathrm{d}E}{\mathrm{d}t} = -\frac{G}{45c^5} \sum_{\alpha,\beta} \left(\frac{\partial^3 D_{\alpha\beta}}{\partial t^3} \right)^2 , \tag{27}$$

where $D_{\alpha\beta}$ is a quadrupole moment tensor of the mass distribution defined to be

$$D_{\alpha\beta} = \int \rho(\mathbf{x}) \, (3x_\alpha x_\beta - r^2 \, \delta_{\alpha\beta}) \, \mathrm{d}\mathbf{x} \, . \tag{28}$$

For our present system of a rigidly rotating ellipsoid of uniform density undergoing nonlinear motions, a straightforward but tedious calculation leads to

$$\begin{aligned} \frac{\mathrm{d}E}{\mathrm{d}t} = -\frac{G}{45c^5} \Big[& \Delta(72\omega^2 \omega^2 + 32\omega^6 - 16\omega^3 \omega + 2\omega^2) + \\ & + \Delta^2(18\omega^2 + 72\omega^4) + \Delta^2(18\omega^2) + \Delta\Delta(12\omega\omega + 96\omega^3 \omega) + \\ & + \Delta\Delta(12\omega\omega - 48\omega^4) + \Delta\Delta(36\omega\omega) - \Delta\Delta(12\omega\omega) - \Delta\Delta(12\omega^2) + \\ & + \sum (D'_{ii})^2 \Big] , \end{aligned} \tag{29}$$

where D'_{ii} is the quadrupole moment tensor calculated with respect to the co-rotating body axes

$$D'_{ii} = \frac{1}{5} M \left(a_i^2 - \sum_{\alpha = 1,\,2,\,3} a_\alpha a_\alpha \right) , \tag{30}$$

ω is the angular velocity given by $\omega = 2L/(a_1 + a_2)^2$ and

$$\Delta = (D'_{11} - D'_{22}) \, . \tag{31}$$

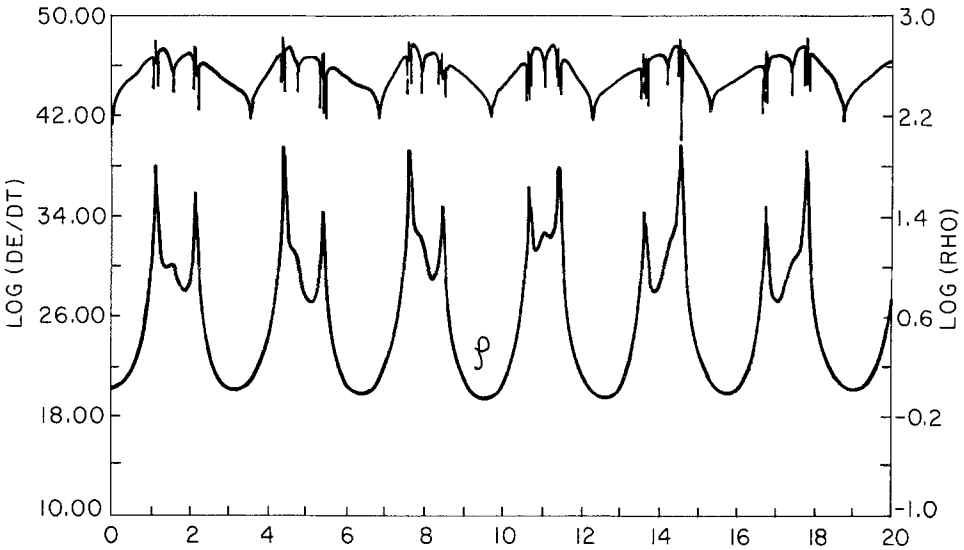

Fig. 5(a). Rate of GR emission and density evolution for axisymmetric collapse with $L = 4.0L_e$, $T_c(0) = 0.111T_{c,e}$, $e(0) = 0.31225$, $k^* = 0$, $M = 1.4\,M_\odot$, $\rho(\text{core}) = 10^9\ \text{g cm}^{-3}$. The units for $d\varepsilon/dt$ are ergs s^{-1}. The units for ρ are $(3M/4\pi a_1^3(0))$, $\rho(0) = 1/a_3^*(0)$. $\tau = 7.08 \times 10^{-2}$ s.

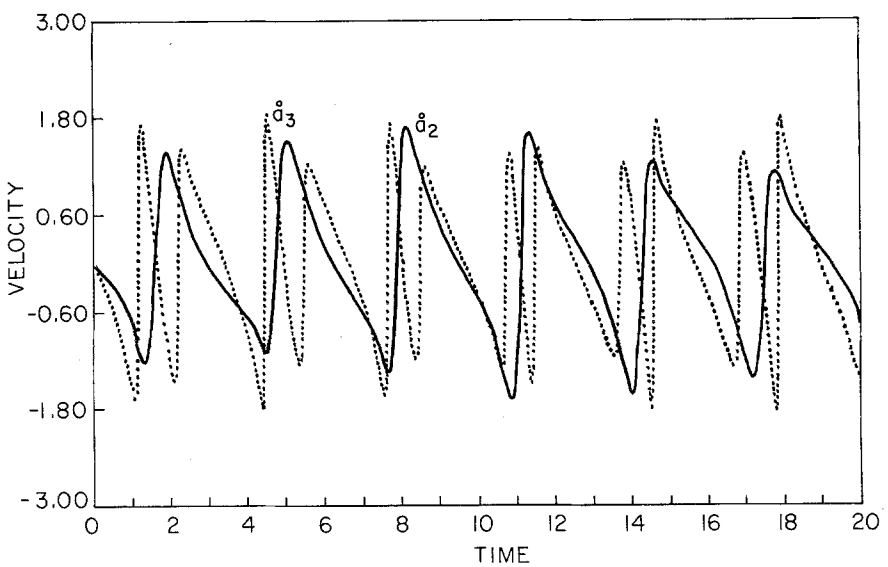

Fig. 5(b). Velocity evolution for axisymmetric collapse with same parameters as in Figure 5(a). Velocities in units of $a_1(0)/\tau$.

The correctness of Equation (29) has been verified by using MACSYMA. Furthermore, it reduces to the well known expression for the axisymmetric case

$$-\frac{dE}{dt} = \frac{26M^2}{375c^5}[a_1 - a_3]^2, \tag{32}$$

as given by, e.g., Thuan and Ostriker (1974); Chia *et al.* (1977), Shapiro (1977); and to

$$-\frac{dE}{dt} = \frac{32}{125}\frac{GM^2\omega^6}{c^5}(a_1^2 - a_2^2)^2 \tag{33}$$

for the case of a rotating ellipsoid in equilibrium, in agreement with the results of Chau (1967).

The loss of angular momentum via gravitational radiation can also be calculated (cf. Peters, 1964) using

$$\frac{dL_i}{dt} = -\frac{26}{45c^5}\sum_{j,m}\varepsilon_{ijk}\ddot{D}_{jm}D_{km}, \tag{34}$$

where L_i is the ith component of the angular momentum vector L and ε_{ijk} is an antisymmetric unit pseudo tensor. The amount emitted, however, is not significant (otherwise our assumption of momentum conservation would not be valid) and in any case, we are far more interested in the energy radiated from the observational point of view.

Equation (29) is now applied to calculate the radiation emitted by a collapsing white dwarf of mass $1.4\,M_\odot$, and initial density of 10^9 g cm^{-3}. As a control check on the numerical scheme, we have been able to recover the results for one of the axisymmetric cases, as reported by Chia *et al.* (1977). In Figures 5(a),5(b), 6(a), 6(b), 6(c) we present the typical results for axisymmetric collapse and then when a small initial non-axisymmetric perturbation is applied. In both cases, $\kappa = 0$. We also present the time-evolution of the density and the velocity of the axes.

The total amount of radiation emitted after 20τ was found to be 9.4×10^{47} ergs for the axisymmetric axes as compared with 1.53×10^{48} ergs for the non-axisymmetric cases. The time-evolution of dE/dt for both cases are initially very similar, and only start to be different when the non-axisymmetric perturbations have time to grow. It is interesting to observe that the maximum rate correlates not just with the moment of maximum density, as expected, but also with the value of $\dot{a}_3$, i.e., the velocity of the axis of rotation. The effects of $\dot{a}_1$ and $\dot{a}_2$ seem to be considerably smaller, a phenomenon that can be understood in terms of the angular momentum terms in the equations of motion. (We also remark that smaller radiation would be expected for systems with larger L because of the centrifugal support against collapse and this is indeed confirmed by our calculations using $L = 4L_e$ for an otherwise identical system.)

The introduction of 'thermal' dissipation would lead to a collapse to higher density and, hence, a larger rate of radiation. Thus while the total amound radiated after 6τ is

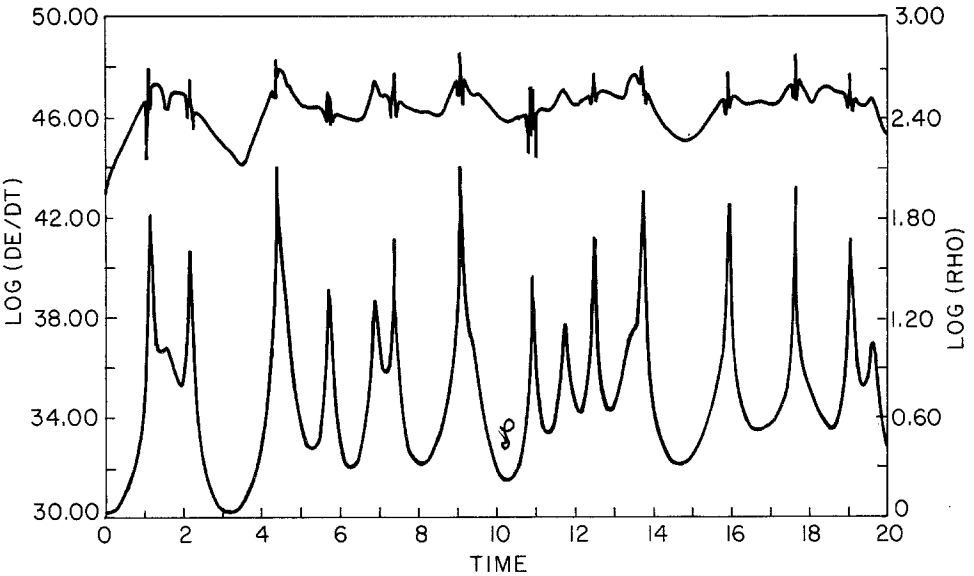

Fig. 6(a). Rate of GR emission and density evolution for non-axisymmetric collapse with $L = 4.0L_e$, $T_c(0) = 0.111T_{c,e}$, $e(0) = 0.31225$, $k^* = 0$, $M = 1.4\,M_\odot$, $\rho_{\text{core}} = 10^9\ \text{g cm}^{-3}$. A small non-axisymmetric perturbation ($\mathrm{d}a_1/\mathrm{d}t(0) = -\mathrm{d}a_2/\mathrm{d}t(0) = 0.04$) has been applied to the equatorial axes. The units for $\mathrm{d}\varepsilon/\mathrm{d}t$ are ergs s^{-1}. The units for ρ are $(3M/4\pi a_1^3(0))$, $\rho(0) = 1/a_3^*(0)$. $\tau = 7 \times 10^{-2}$ s.

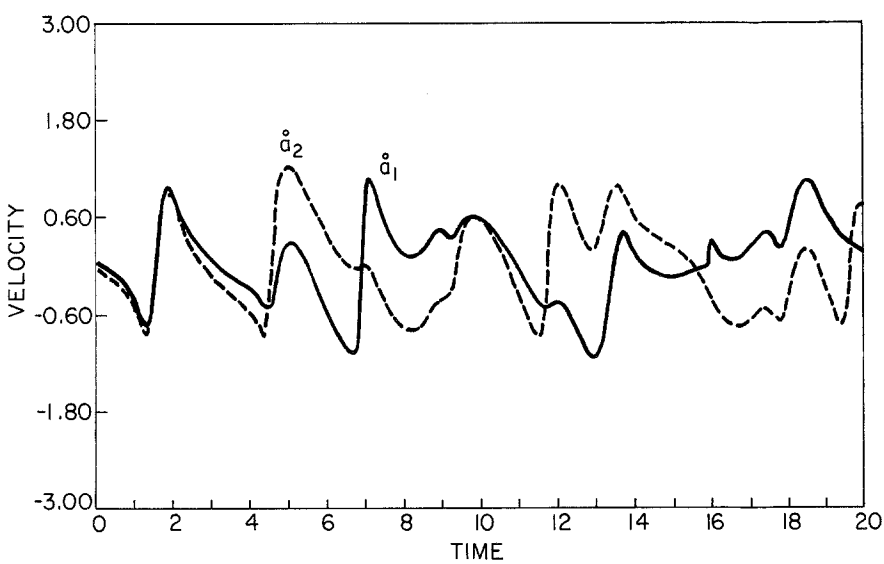

Fig. 6(b). Time-evolution of the velocities of the equatorial axes for the non-axisymmetric collapse of Figure 6(a).

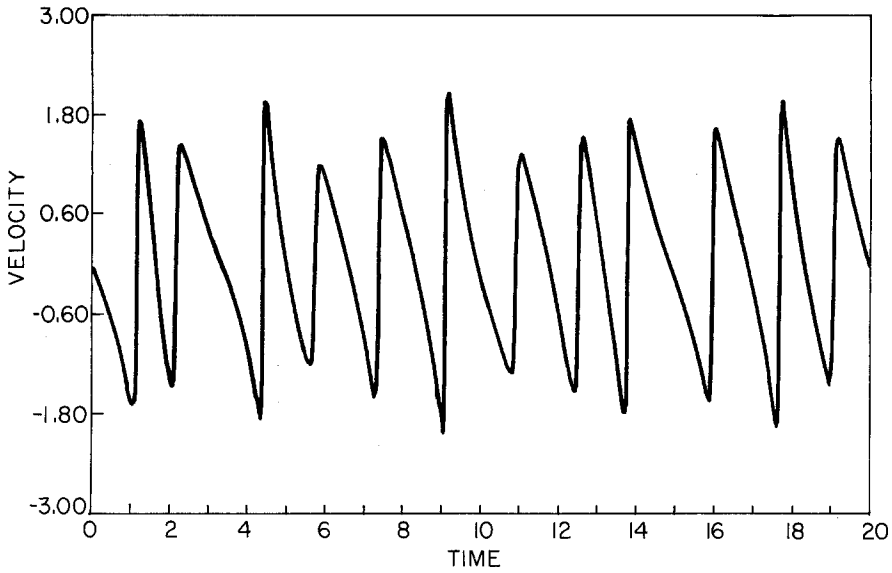

Fig. 6(c). Time-evolution of the velocity $\dot{a}_3$ for the non-axisymmetric collapse of Figure 6(a).

4.6×10^{47} ergs for the non-axisymmetric case presented in Figures 6(a) and 6(b), it is found to be 1.38×10^{48} ergs when we take $\kappa = 0.01$. We must remark that though the rate is higher for the non-adiabatic case, the system can bounce much longer when $\kappa = 0$. Also, $\kappa = 0.01$ corresponds to a thermal energy loss of 3.9×10^{52} ergs at 6τ, hence completely dominating over GR in affecting the dynamics of the system.

As explained earlier, we do not expect the radiation to be important for the cases of explosion. Indeed, we found that the amounts are typically down by 3–4 orders of magnitude when the same configuration was made to explode. We also would not expect any significant radiation from exploding/collapsing galactic size objects because of the small density involved.

4.2. Angular, polarization dependence, and wave forms

While the amount of energy radiated is certainly of interest from the observational point of view, of at least equal importance is a study of the detailed polarization dependence and wave forms of the radiation. This could yield ready information on the nature of the motion of the source and can even be used to discriminate between different rival theories of gravitation.

The intensity of radiation of a given polarization per unit solid angle Ω for waves propagating in the direction of the unit vector $\mathbf{n}$ is given by Landau and Lifshitz (1975) as

$$\frac{dI}{d\Omega} = \frac{G}{72\pi c^5} (D_{\alpha\beta} e_{\alpha\beta})^2 , \tag{35}$$

where $e_{\alpha\beta}$ is the three-dimensional unit polarization tensor of the plane gravitational wave satisfying the following conditions

$$\Sigma\, e_{\alpha\alpha} = 0\,, \qquad \Sigma\, n_\beta e_{\alpha\beta} = 0\,, \qquad \Sigma\, e_{\alpha\beta} e_{\alpha\beta} = 1\,. \tag{36}$$

For definiteness in the calculation, $\mathbf{n}$ is specified by the usual polar angle θ and azimuth ϕ, with the inertial axis centered on the source such that X_3 is along the axis of rotation. The two independent polarization modes are then given by (Landau and Lifshitz, 1975)

$$e_{\phi\theta} = \frac{1}{\sqrt{2}}\,; \qquad e_{\theta\theta} = -e_{\phi\phi} = \frac{1}{\sqrt{2}}\,. \tag{37}$$

Using the expressions that we have for the mass quadrupole tensor appropriately projected along the θ–ϕ directions

$$\begin{aligned} D_{\theta\phi} &= \cos\theta\{\tfrac{1}{2}\sin 2\phi(D_{22} - D_{11}) + D_{12}\cos 2\phi\}\,, \\ D_{\theta\theta} &= \cos^2\theta(D_{11}\cos^2\phi + D_{22}\sin^2\phi) + D_{12}\cos^2\theta\sin 2\phi + D_{33}\sin^2\theta\,, \\ D_{\phi\phi} &= D_{11}\sin^2\phi + D_{22}\cos^2\phi - D_{12}\sin 2\phi\,; \end{aligned} \tag{38}$$

and averaging over ϕ, we have after a long, tedious calculation the expressions for the energy in the two polarization modes

$$\frac{\mathrm{d}I_1}{\mathrm{d}\Omega} = \frac{G}{72\pi c^5}\,[\tfrac{1}{4}(D_{22} - D_{11})^2 + D_{12}^2]\cos^2\theta \tag{39}$$

and

$$\begin{aligned} \frac{\mathrm{d}I_2}{\mathrm{d}\Omega} = \frac{G}{144\pi c^5}\,\{&\cos^4\theta(\tfrac{3}{8}(D_{11}^2 + D_{22}^2 + \tfrac{1}{2}D_{12}^2 + 2D_{33}^2 + \tfrac{1}{4}D_{11}D_{22}) + \\ &+ \cos^2\theta(D_{12}^2 - \tfrac{1}{4}(D_{11}^2 + D_{22}^2) - 4D_{33}^2 - \tfrac{3}{2}D_{11}D_{22}) + \\ &+ \tfrac{3}{8}(D_{11}^2 + D_{22}^2) + \tfrac{1}{2}D_{12}^2 + 2D_{33}^2 + \tfrac{1}{4}D_{11}D_{22}\}\,. \end{aligned} \tag{40}$$

As an accuracy check, Equations (39) and (40) reduce to known expressions for simpler situations, e.g., two-point masses in circular orbit (Landau and Lifshitz, 1975). Also after integration over all angles we recover the rate of GR emission for a rotating ellipsoid and non-radially pulsating sphere (Chau, 1967) and axisymmetric collapse/explosion (Chia *et al.*, 1977; Shapiro, 1977). In addition, the sum of (39) and (40) should give the total radiation (summed over all polarization rates) per unit solid angle, and the results agree with an independent calculation using (Landau and Lifshitz, 1975)

$$\frac{\mathrm{d}I}{\mathrm{d}\Omega} = \frac{G}{36\pi c^5}\sum_{\alpha,\beta}\,[\tfrac{1}{4}(D_{\alpha\beta}n_\alpha n_\beta)^2 + \tfrac{1}{2}D_{\alpha\beta}^2 - D_{\alpha\beta}D_{\alpha\gamma}n_\beta n_\gamma]\,. \tag{41}$$

Furthermore, the *total* energy in each polarization mode can be simply obtained by integrating over all angles. Thus for the $e_{\theta\phi}$ mode for example, we have

$$I_1 = \int \frac{dI_1}{d\Omega}\, d\Omega = \frac{G}{54c^5}\,[\tfrac{1}{4}(D_{22} - D_{11})^2 + D_{12}^2]\,. \tag{42}$$

The other property of the wave that provides a clue on the dynamics of the source is the wave form of the radiation. For a stationary observer located at (r, θ, ϕ) with respect to a fixed (X_1, X_2, X_3) axis centered on the source, we have for large r (Landau and Lifshitz, 1975)

$$h_{\phi\theta} = -\frac{2G}{3c^4 R_0}\,\ddot{D}_{\theta\phi}\,, \tag{43}$$

$$h_{\theta\theta} = -h_{\phi\phi} = -\frac{G}{3c^4 R_0}\,(\ddot{D}_{\theta\theta} - \ddot{D}_{\phi\phi})\,, \tag{44}$$

which can then be readily evaluated using Equations (38) for the $D_{\theta\phi}$'s, leading to the results obtained by Saenz and Shapiro (1979).

The above expressions are applied to the collapsing white dwarf configurations as already discussed, for both the axisymmetric and the nonaxisymmetric situations. It is immediately obvious that for the axisymmetric case $dI_1/d\Omega$ and $h_{\theta\phi}$ are identically zero, hence, all the radiation is omitted in only *one* polarization mode. We plot in Figure 7 the wave form $h_{\theta\phi}$ as a function of time for the axisymmetric case. Also plotted on

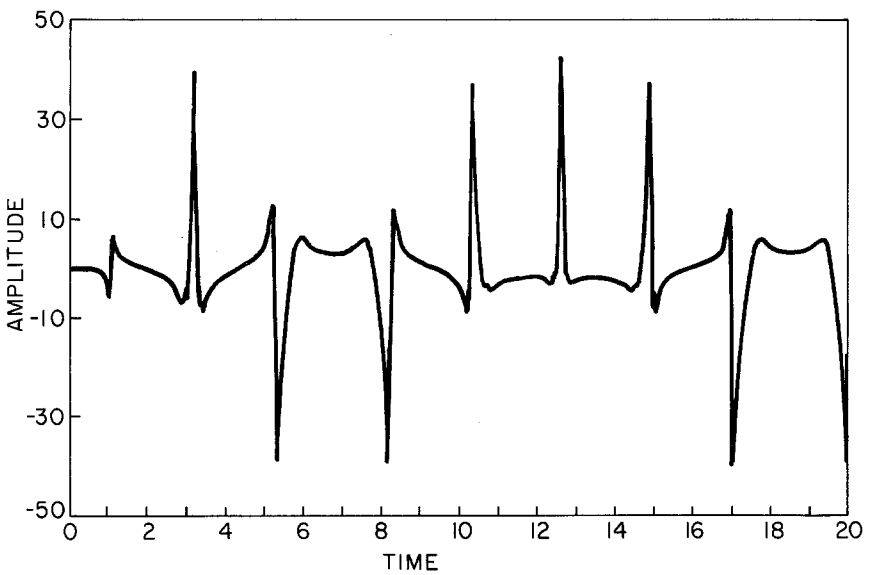

Fig. 7. Wave amplitude evolution for axisymmetric collapse. The initial parameters are $L = 1.0L_e$, $T_c(0) = 0.111T_{c,e}$, $e(0) = 0.31225$, $k^* = 0$. Time is in units of τ. Amplitude is in units of $M \sin^2\theta/5R$.

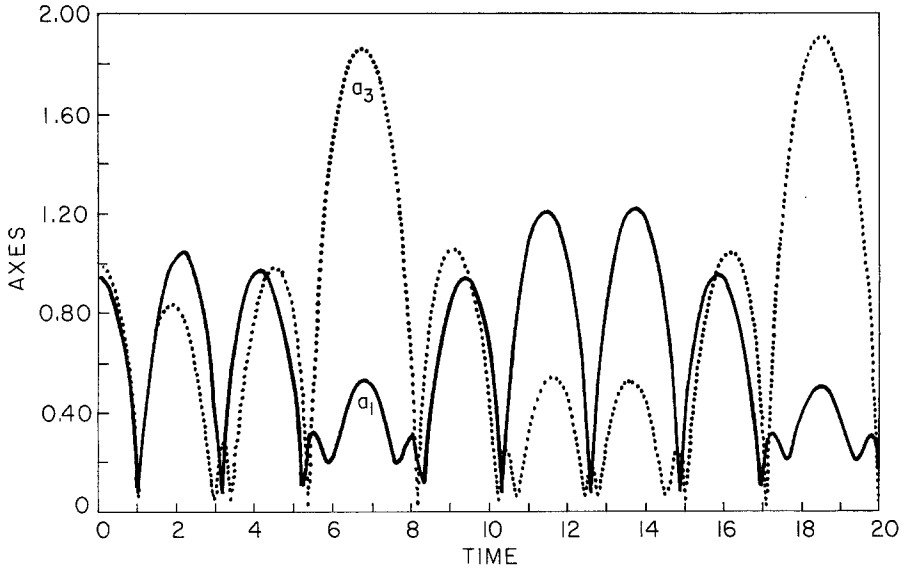

Fig. 8. Evolution of the semi-axes of collapsing configuration for the same parameters as in Figure 7. Axes in units of $a_1(0)$.

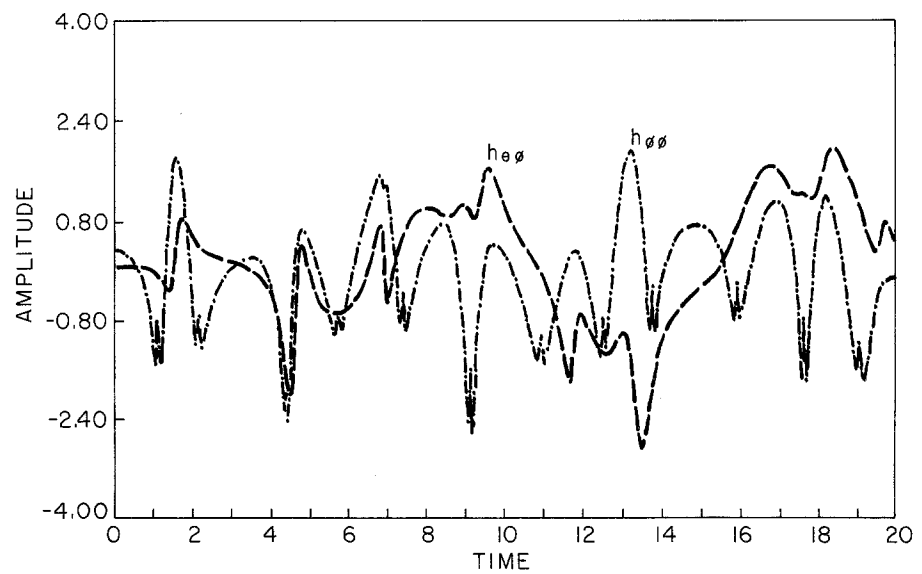

Fig. 9. $h_{\theta\phi}$ ($\phi = 0$) and $h_{\phi\phi}$ ($\phi = \pi/2$) for non-axisymmetric collapse with $L = 4.0L_e$, $T_c(0) = 0.111T_{c,e}$, $e(0) = 0.31225$, $k = 0$. A small non-axisymmetric perturbation ($da_1/dt = -da_2/dt = 0.04$) has been applied. Amplitude is in units of M/R.

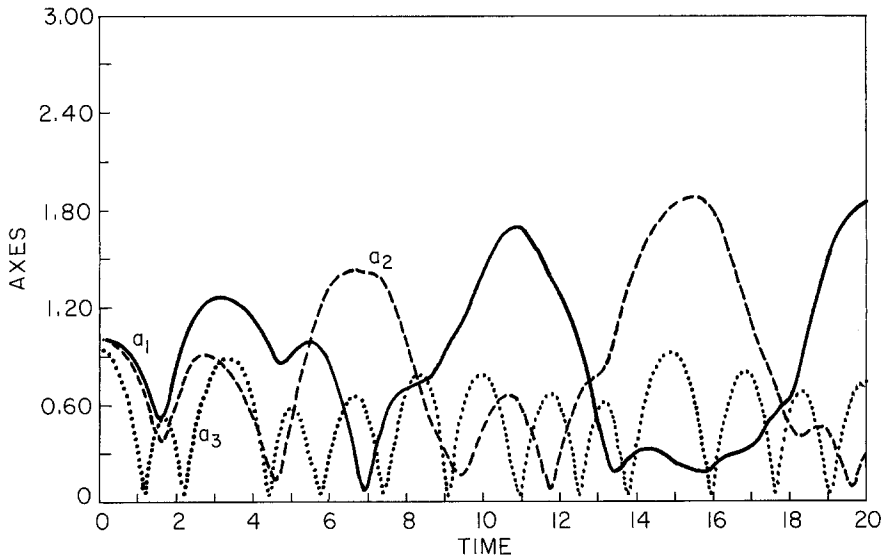

Fig. 10. Non-axisymmetric collapse for the configuration described in Figure 9. Axes in units of $a_1(0)$.

Figure 8 are the time-evolution of the axes a_1 and a_3. It is immediately clear that the peaks correspond to bounces along the two different axes, with positive peaks correlating with bounces on the equatorial plane and negative peaks with those of the rotational axis. We remark that from a source like this located at the Virgo Cluster (~ 20 MPc away), we have $h \sim 10^{-20}$–10^{-22}, in close agreement with those given by Shapiro (1979), considering the difference in the equation of state used and the difference in the numerical scheme.

The corresponding results for non-axisymmetric collapse are presented in Figure 9 for $h_{\phi\phi}$ and $h_{\theta\phi}$. The time-evolution of the axes is presented in Figure 10. It can be seen that $h_{\theta\phi}$ is a much more slowly varying function of time than $h_{\theta\theta}$. Furthermore, we note the different correlation between the wave amplitude and the motion along the axes for the different polarization modes. Whereas $h_{\phi\phi}$ correlates with the bounces along X_3, and to a smaller extent also along X_1 and X_2, similar to the axisymmetric case, the amplitude in $h_{\theta\phi}$ correlates principally with bounces in a_1 and a_2. This affords additional clues on the nature of the motion of the source.

5. Summary and Conclusions

The nonlinear motion (collapse and explosion) of a rigidly rotating, gaseous ellipsoid of uniform density has been thoroughly studied with and without the additional effects of an external halo. The properties of the gravitational waves emitted are also delineated.

The case of non-axisymmetric collapse is of interest in that the 'final' configuration could be a long, elongated bar-shaped one. This leads to a substantial increase

(~ several times) in the amount of gravitational radiation, in addition to potential, significant implications for morphology of star formation regions, origin of barred galaxies and close binaries. Viscosity dissipation should be incorporated in further extension of this work, as well as a more realistic cooling law for the collapsing system.

The possibility of an invisible halo surrounding many galaxies, especially spirals, adds credibility to our model for the halo (despite the apparently restrictive assumptions) and potential significance for the results. The strong focussing property of such an external gravitational field comes out clearly from our calculations. To allow for a more realistic and general application, the effects of ram pressure must be allowed for in future work (see, e.g., Saenz and Shapiro, 1981).

A detailed study of the wave forms and angular polarization dependence of the radiation reveals information on the nature of the source. While the amount of radiation is about the same for *both* the axisymmetric and non-axisymmetric case, there is a big, qualitative difference in the polarization pattern, namely, only one polarization state for axisymmetric motion as compared with two for the other case. There are also differences in the correlation of the wave amplitude to the motion along different axis. This should contribute to the *Catalogue of Wave Forms* suggested by Thorne and Braginsky (1976) as a guide for designing future wave detectors.

Further to the results summarized above, the basic formulation of the problem together with the relatively simple and efficient numerical scheme (made possible by the special properties of the potential functions) should provide an attractive first step in the study of various diverse problems like star formation, galaxy formation, morphology of radio jets and the evolution of voids in the early universe.

Acknowledgements

The research is partially supported by an Operating Grant from the Natural Sciences and Engineering Research Council (Canada) to one of the authors (WYC). We also acknowledge the generosity of Dr K. Lake for following us access to his MACSYMA account at M.I.T. H.B. thanks the financial support of Queen's University while this research was carried out, and we also thank Prof. J.-L. Zhang for helpful discussions in the course of this work.

References

Bock, B.: 1977, *Publ. Astron. Soc. Pacific* **89**, 597.
Bodenheimer, P. and Black, D. C.: 1978, in T. Gehrels (ed.), *Protostars and Planets*, University of Arizona Press, Tucson.
Chan, K. L., Chau, W. Y., and Henriksen, R. N.: 1978, *Astrophys. J.* **225**, 625 (Paper I).
Chan, K. L., Chau, W. Y., and Henriksen, R. N.: 1980, *Astrophys. J.* **236**, 889.
Chandrasekhar, S.: 1969, *Ellipsoidal Figures of Equilibrium*, Yale University Press, New Haven.
Chandrasekhar, S. and Lebovitz, N.: 1962, *Astrophys. J.* **136**, 1037.
Chau, W. Y.: 1967, *Astrophys. J.* **147**, 664.
Chia, T. T., Chau, W. Y., and Henriksen, R. N.: 1977, *Astrophys. J.* **214**, 576.
Durisen, R. H.: 1978, *Astrophys. J.* **224**, 26.

Field, G. B.: 1978, in T. Gehrels (ed.), *Protostars and Planets*, University of Arizona Press, Tucson.
Fujimoto, M.: 1968, *Astrophys. J.* **152**, 623.
Henriksen, R. N., Chau, W. Y., and Chan, K. L.: 1979,
Landau, L. and Lifshitz, E.: 1975, *The Classical Theory of Fields*, Pergamon Press, London.
Martin, R. N. and Barret, A. H.: 1978, *Astrophys. J. Suppl.* **36**, 1.
Myers, P. C.: 1983, *Astrophys. J.* **270**, 105.
Novikov, I. D.: 1975, *Soviet Astron.* **19**, 398.
Peters, P. C.: 1964, *Phys. Rev.* **136**, 1229.
Rubin, V.: 1983, *Science* **220**, 1339.
Saenz, R. A. and Shapiro, S. L.: 1978, *Astrophys. J.* **221**, 286.
Saenz, R. A. and Shapiro, S. L.: 1979, *Astrophys. J.* **229**, 1107.
Saenz, R. A. and Shapiro, S. L.: 1981, *Astrophys. J.* **244**, 1033.
Shapiro, S. L.: 1977, *Astrophys. J.* **214**, 566.
Thorne, K. S. and Braginsky, V.: 1976, *Astrophys. J.* **191**, L105.
Thuan, T. X. and Ostriker, J. P.: 1974, *Astrophys. J.* **191**, L107.